



RESEARCH ARTICLE

10.1029/2023EF004300

Key Points:

- We quantify how the ARISE-SAI controller responds to different patterns of internal variability
- The impact from internal variability on the controller-determined injection is dependent on the background warming
- This method provides a straightforward way to efficiently quantify controller sensitivity to internal variability

Supporting Information:

Supporting Information may be found in the online version of this article.

Correspondence to:

C. Connolly, cconn@rams.colostate.edu

Citation:

Connolly, C., Prewett, E., Barnes, E. A., & Hurrell, J. W. (2024). Quantifying the impact of internal variability on the CESM2 control algorithm for stratospheric aerosol injection. *Earth's Future*, *12*, e2023EF004300. https://doi.org/10.1029/2023EF004300

Received 22 DEC 2023 Accepted 20 MAY 2024

Quantifying the Impact of Internal Variability on the CESM2 Control Algorithm for Stratospheric Aerosol Injection

Charlotte Connolly , Emily Prewett , Elizabeth A. Barnes, and James W. Hurrell , and James W. Hurrell

¹Department of Atmospheric Science, Colorado State University, Fort Collins, CO, USA

Abstract Earth system models are powerful tools to simulate the climate response to hypothetical climate intervention strategies, such as stratospheric aerosol injection (SAI). Recent simulations of SAI implement a tool from control theory, called a controller, to determine the quantity of aerosol to inject into the stratosphere to reach or maintain specified global temperature targets, such as limiting global warming to 1.5°C above preindustrial temperatures. This work explores how internal (unforced) climate variability can impact controller-determined injection amounts using the Assessing Responses and Impacts of Solar climate intervention on the Earth system with Stratospheric Aerosol Injection (ARISE-SAI) simulations. Since the ARISE-SAI controller determines injection amounts by comparing global annual-mean surface temperature to predetermined temperature targets, internal variability that impacts temperature can impact the total injection amount as well. Using an offline version of the ARISE-SAI controller and data from Earth system model simulations, we quantify how internal climate variability and volcanic eruptions impact injection amounts. While idealized, this approach allows for the investigation of a large variety of climate states without additional simulations and can be used to attribute controller sensitivities to specific modes of internal variability.

Plain Language Summary Stratospheric aerosol injection (SAI) is a proposed climate intervention strategy that injects aerosols into the stratosphere to mitigate some climate change impacts. Several studies that have used climate models to investigate how the atmosphere may respond to SAI implement control algorithms to determine how much aerosol to inject and where in order to achieve certain climate targets. This work explores how changes to the controller input can impact the amount of aerosol injected. Here we focus on the controller from the Assessing Responses and Impacts of Solar climate intervention on the Earth system with Stratospheric Aerosol Injection (ARISE-SAI) simulations. This specific controller uses the annual-mean surface temperature to determine how much aerosol to inject. Therefore, internal variability that impacts temperature can impact the total injection amount as well. To quantify how patterns of internal variability impact how much aerosol is injected, we isolate the ARISE-SAI controller and pass a variety of temperature patterns into it. While this method ignores some interactions between the controller and the climate simulation, it is a quick way to quantify the controller's sensitivity to a large variety of temperature patterns without additional simulations.

1. Introduction

Current actions and plans by global nations to reduce greenhouse gas emissions may not be enough to keep global warming under 2° C (Liu & Raftery, 2021; Raftery et al., 2017). Climate intervention strategies have been proposed as a solution to reduce some of the negative consequences associated with climate warming (Cicerone, 2006; Crutzen, 2006; NASEM, 2021). One such proposed strategy, called stratospheric aerosol injection, injects aerosols or their precursors into the stratosphere to reflect a small percentage of incoming solar radiation. Many studies simulate the injection of sulfur dioxide (SO₂), which oxidizes into reflective sulfate aerosols. This approach has been motivated by observed global cooling after certain volcanic eruptions that inject SO₂ into the lower stratosphere (NASEM, 2021).

Several modeling projects have been conducted to understand how the climate system may respond to additional SO_2 in the stratosphere (Kravitz et al., 2013, 2015; Rasch et al., 2008; Richter et al., 2022; Tilmes et al., 2018). Some of these simulations implement a feedback algorithm, called a controller, which determines how much aerosol to inject into the stratosphere to maintain the climate system at pre-established temperature targets (MacMartin et al., 2014; Richter et al., 2022; Tilmes et al., 2018).

© 2024. The Author(s). This is an open access article under the terms of the Creative Commons Attribution License, which permits use, distribution and reproduction in any medium, provided the original work is properly cited.

CONNOLLY ET AL. 1 of 10



The Assessing Responses and Impacts of Solar climate intervention on the Earth system with Stratospheric Aerosol Injection (ARISE-SAI) simulations, performed with version two of the Community Earth System Model (CESM2; Danabasoglu et al., 2020), implement a controller to keep global mean surface temperature near 1.5°C while also maintaining temperature gradients so that atmospheric circulations are minimally impacted (Richter et al., 2022). The controller accomplishes this by comparing the global temperature (T0), the north-south temperature gradient (T1) and the Equator-to-pole temperature gradient (T2) to predetermined targets of 288.64, 0.8767, and -5.89 respectively (Kravitz et al., 2017). Deviations between the T0, T1, and T2 values calculated from model output and the individual predetermined targets are used by the controller to determine how much SO₂ to inject at four different locations (30°N, 15°N, 15°S, 30°S).

In the ARISE-SAI simulations, the controller impacts the climate system by determining how much SO_2 is needed to maintain the climate system at the pre-determined targets. Additionally, since the controller determines injection amounts based on deviations of T0, T1, and T2 from their respective targets, global and regional temperature patterns driven by internal climate variability can impact injection amounts. A handful of studies have begun to explore how the controller and the simulated climate system impact one another. For example, Mac-Martin et al. (2014) show that the way in which the controller is tuned and the lag between the controller input and the response of the system can impact the internal variability of the climate system. Diao et al. (2023) use data from the ARISE-SAI simulations to show that ENSO accounts for 70% of the year-to-year variability in injection anomalies determined by the controller. In this work, we further explore how internal variability and volcanic eruptions impact SO_2 injection by passing global temperature maps with different internal variability patterns into an offline version of the ARISE-SAI controller.

2. Methods

The ARISE-SAI controller's sensitivity to internal variability is quantified by creating controller inputs, where the warming pattern and the patterns of internal variability are known. These controller inputs are then passed to the controller. The way in which the warming patterns and patterns of internal variability are calculated is provided in Section 2.1. An offline version of the ARISE-SAI controller is used to explore a large range of climate states without having to run additional simulations, and details about the changes made to the ARISE-SAI controller are in Section 2.2.

2.1. Controller Inputs

The 10 member ARISE-SAI control simulation (ARISE-SAI-CTRL) is used to create the controller inputs (Richter et al., 2022). The ARISE-SAI-CTRL comes from the same model configuration the ARISE-SAI controller was tuned for but does not contain any SAI. Using the ARISE-SAI-CTRL means thats the controller inputs will not contain any SAI driven cooling.

Every controller input map contains one forced component which describes the climate warming trend. The forced component is defined as the smoothed annual-mean ensemble mean near surface temperature using years 2035–2070 from the ARISE-SAI-CTRL. However, since 10 members are not enough to remove all internal variability (Deser et al., 2012), the ensemble mean is smoothed by fitting a third order polynomial to the time series at each grid point. These smoothed data are used as the *base states*, and we focus on the years 2035 and 2045 in this study. The year 2035 defines when SAI begins in ARISE-SAI. Year 2045 defines when SAI begins in a different set of simulations which are designed to inform about the atmospheric responses after a delayed deployment using the same AIRSE-SAI temperature targets (MacMartin et al., 2022).

Unforced components, or *internal variability patterns*, are defined as monthly temperature anomalies composited based on internal variability events. Any number of internal variability patterns of interest can be added onto a base state to quantify their impacts on total injection amounts. This work focuses on variability associated with the El-Niño Southern Oscillation (ENSO; Trenberth, 1997), the Southern Annular Mode (SAM; Ho et al., 2012), the North Atlantic Oscillation (NAO; Hurrell, 1996), and the eruption of Mt. Pinatubo (Holasek et al., 1996). These modes of variability are selected because each produces strong temperature anomalies in different regions of the globe. ENSO influences temperature predominantly at low latitudes, the NAO influences temperature at the high latitudes of the Northern Hemisphere, the SAM influences temperature the high latitudes of the Southern Hemisphere, and a Pinatuno-like volcanic eruption influences temperatures globally.





The aforementioned internal variability patterns are created by compositing maps of temperature anomalies based on each climate index. The temperature anomalies are calculated by subtracting the smoothed ensemble mean from each ensemble member and removing the seasonal cycle. Monthly temperature anomalies are used instead of annual to increase the amount of the data that goes into each composite. To enhance the robustness of the results, anomalies from years 2035–2070 from the 100 member CESM2 Large Ensemble historical simulation (CESM2-LE; Rodgers et al., 2021) are also analyzed. While ARISE-SAI utilizes a moderate emissions scenario and CESM2-LE utilizes a moderate to high emissions scenario, we show that our conclusions are not impacted by this difference (Riahi et al., 2017).

The climate indices used to composite temperature anomalies associated with ENSO, NAO, and SAM events are calculated using sea surface temperature and sea level pressure from the ARISE-SAI-CTRL and the CESM2-LE. Methods used to calculate each climate index are as follows:

- 1. The ENSO index is defined by the Nino3.4 index (Trenberth, 1997) based on the five month average sea surface temperature within the 5°N–5°S, 120–170°W region. A positive ENSO event is characterized by warmer than average temperatures in central and eastern Tropical Pacific and a negative ENSO has cooler than average temperatures (Trenberth, 1997).
- 2. The NAO index is defined by the principal component time series of the leading empirical orthogonal function of surface pressure anomalies within 20–80°N, 90°W–40°E (Hurrell & Deser, 2010). When the NAO is positive, sea level pressures are anomalously low over the subpolar North Atlantic. The opposite occurs during the negative phase of the NAO. The sea level pressure anomalies drive circulation responses that impact regional temperature patterns in a variety of ways (e.g., Hanna & Cropper, 2017; Hurrell & Deser, 2010; Riviére & Drouard, 2015). For example, when the NAO is in its negative state it drives warmer than average temperatures across Northern Europe (Fuentes-Franco et al., 2023).
- 3. The SAM index is calculated as the principal component of the leading empirical orthogonal function of sea level pressure over the region 20–90°S (Ho et al., 2012). When the SAM is positive, sea level pressures over the Southern Hemisphere polar region are anomalously low and temperatures are cooler than average. However, when the SAM is negative, sea level pressures are anomalously high and temperatures are warmer than average (e.g., Fogt & Marshall, 2020; Gillett et al., 2006).

The temperature anomaly pattern associated with the Mt. Pinatubo eruption is defined as the average temperature anomaly two years following the eruption (June 1991–June 1993). The 100 member CESM2-LE climate warming trend is estimated by fitting a line at every grid point to the ensemble mean surface temperature anomalies time series 10 years prior to the eruption (May 1981–May 1991). This line is extrapolated to June 1993, two years following the eruption, and then subtracted from the ensemble mean. Assuming the internal variability is removed by calculating the ensemble mean of 100 members and that the linear fit represents a short term continued warming trend, subtracting the linear fit from the ensemble mean estimates the temperature anomalies associated with the eruption of Mt. Pinatubo. Figure S1 in the Supporting Information S1 demonstrates an example of fitting a line to calculate temperate anomalies associated with Mt. Pinatubo.

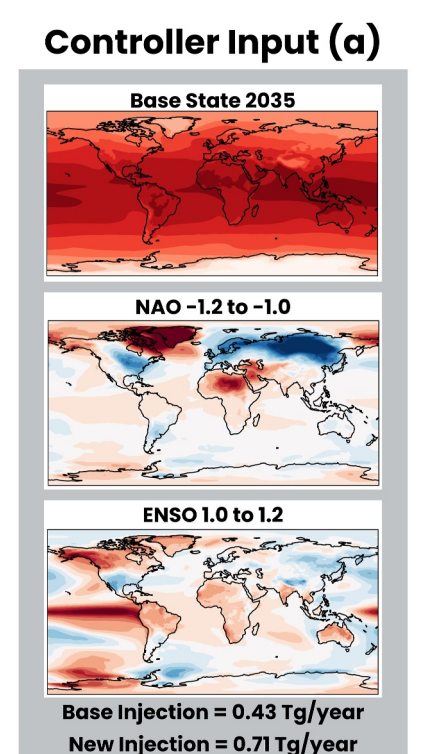
2.2. Changes to the Controller

The ARISE-SAI controller is a proportional-integral control algorithm, or PI controller (Astrom & Murray, 2021). With a PI controller, the proportional term accounts for the current error between model output and the predetermined targets and the integral term accounts for any persistent errors in time. Constants, called gains, are tuned to determine how much of each component is needed to maintain the system at the user-specified targets (Astrom & Murray, 2021; Jarvis & Leedal, 2012; MacMartin et al., 2014). The active controller in the ARISE-SAI simulations has a ramp up time of 5 years, which reduces shock to the system, and considers errors from previous years in the calculation via the integral portion of the controller. More details about the complete ARISE-SAI simulations and its active controller can be found in Richter et al. (2022) and Kravitz et al. (2017) and the sources within. This work utilizes an offline version of the ARISE-SAI controller where the gain values are kept the same (i.e., no addition tuning) and the controller is not connected to an active simulation.

Some additional changes are made to the offline ARISE-SAI controller for this work. First, since the offline controller is not connected to a simulation and cannot shock the simulated climate system by suddenly injecting large amounts of SO₂, the ramp-up period is reduced from 5 years to 1 year. Second, the offline controller only receives one input at a time; therefore the controller does not have errors from previous years to use when



23284277, 2024, 6, Downloaded from https://agupubs.onlinelibrary.wiley.com/doi/10.1029/2023EF004300 by Colorado State University, Wiley Online Library on [01/11/2024]. See the Terms and Conditions



Percent Change = 65.1%

Controller Input (b)

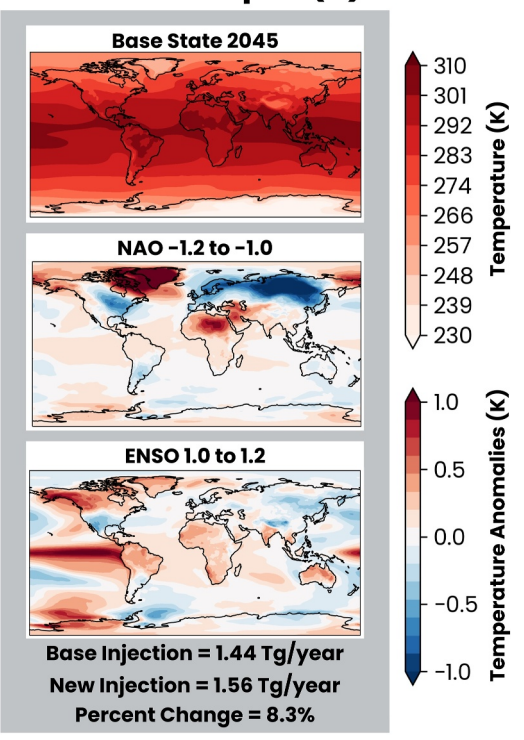


Figure 1. Schematic showing patterns that make up two different controller inputs. For controller input (a), the patterns associated with an North Atlantic Oscillation (NAO) index between -1.2 and -1.0 and El-Niño Southern Oscillation (ENSO) index between 1.0 and 1.2 are added onto the 2035 base state. The same patterns of internal variability are added onto the 2045 base state to create controller input (b). The base injection is the amount injected given only the base state while the new injection is the injection amount when all components are summed. Percent change shows how much internal variability changes the total injection as a function of the base state.

calculating an injection amount for the current input. These changes ensure that when a temperature pattern is fed through the controller, the injection amount is determined by a single temperature pattern and not an evolving state.

3. Results

The total injection when only the base states are passed into the controller quantifies the total injection in response to the climate warming signal. For the base states of 2035 and 2045, the injections are 0.43 Tg/year and 1.44 Tg/year, respectively (Figure 1). Next, different combinations of internal variability patterns are added onto these base states to create new controller inputs that, when passed into the controller, quantify the impact of internal variability on the total injection amounts.

Figure 1 shows how the controller responds to the same patterns of internal variability occurring under different background warming. The difference between the 2035 base state and 2045 base state is found in Supporting Information S1 in the Figure S2. Controller input (a) in Figure 1 shows the base state from 2035, the temperature anomaly pattern associated with na Enso index between 1.0 and 1.2, and the temperature anomaly pattern associated with NAO index between -1.2 and -1.0. When these three patterns are added together and then passed into the controller, the controller injects 0.71 Tg/year of SO_2 into the stratosphere. Adding the same internal variability patterns onto the base state 2045 (controller input (b)), the total injection increases to 1.56 Tg/year. The two patterns of internal variability shown in Figure 1 are responsible for increasing the total injection by 0.28 Tg/year in 2035 and by 0.12 Tg/year in 2045. These increases are similar in magnitude, but in relation to the base injection (i.e., percent change), the patterns of internal variability have a greater impact in 2035 than 2045: 65.1% increase compared to a 8.3% increase. This shows the amount of SO_2 injected in response to internal variability in 2045. In the



23284277, 2024, 6, Downloaded from https://agupubs.onlinelibrary.wiley.com/doi/10.1029/2023EF004300 by Colorado State University, Wiley Online Library on [01/11/2024]. See the Terms and Conditions (https://or

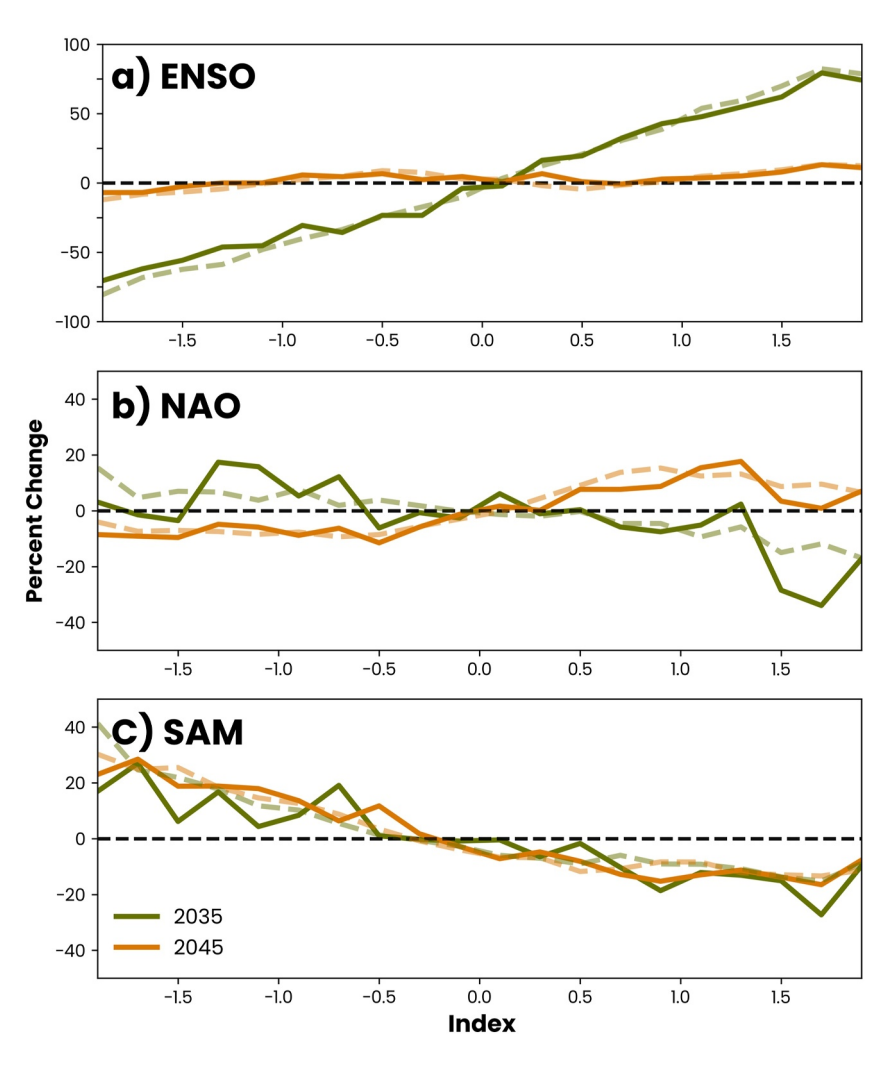


Figure 2. Percent change in total SO₂ injection as a function of (a) El-Niño Southern Oscillation (ENSO), (b) North Atlantic Oscillation (NAO), and (c) Southern annular mode (SAM) events. Solid lines use data from ARISE-SAI-CTRL and dashed lines use data from CESM2-LE. Green lines use year 2035 base state and orange lines use year 2045 base state. Black dashed line marks zero percent change.

following analysis, we add different combinations of internal variability patterns onto each base state (see Supporting Information S1 in the Figure S3 for what climate indices are used in each figure).

Since the impacts from internal variability on the controller-determined total injection depends on the base state, the ENSO, NAO, and SAM impacts on the total injection amounts are quantified as percent changes in Figure 2 (see Supporting Information S1 in the Figure S4 for total change). The percent change is calculated as the change in injection amount divided by the base injection amount (Figure 1). In Figure 2, positive ENSO events are shown to increase the amount of SO_2 injected and negative ENSO events decrease the amount SO_2 injected (Figure 2a), since positive ENSO events are shown to increase the global average temperature and negative events do the opposite (Angell, 1990). The stronger the ENSO event, the greater the impact on the total injection, although, the impact of ENSO anomalies on the controller decreases substantially from year 2035 to year 2045. This is because as the climate warming signal increases, the ENSO internal variability pattern is a smaller percentage of the input and thus a smaller role in the total injection amount.

The NAO has a smaller impact on the total injection in 2035 when compared to ENSO and its impact switches signs from 2035 to 2045. The SAM also has a smaller impact on the total injection than ENSO but its impact doesn't change from 2035 to 2045. Similar SAM and NAO impacts exist in both the ARISE-SAI-CTRL and CESM2-LE data and are therefore not a result of noise in the composites but a response to the internal variability

23284277, 2024, 6, Downloaded from https://agupubs.onlinelibrary.wiley.com/doi/10.1029/2023FE004300 by Colorado State University, Wiley Online Library on [01/11/2024]. See the Terms and Conditions

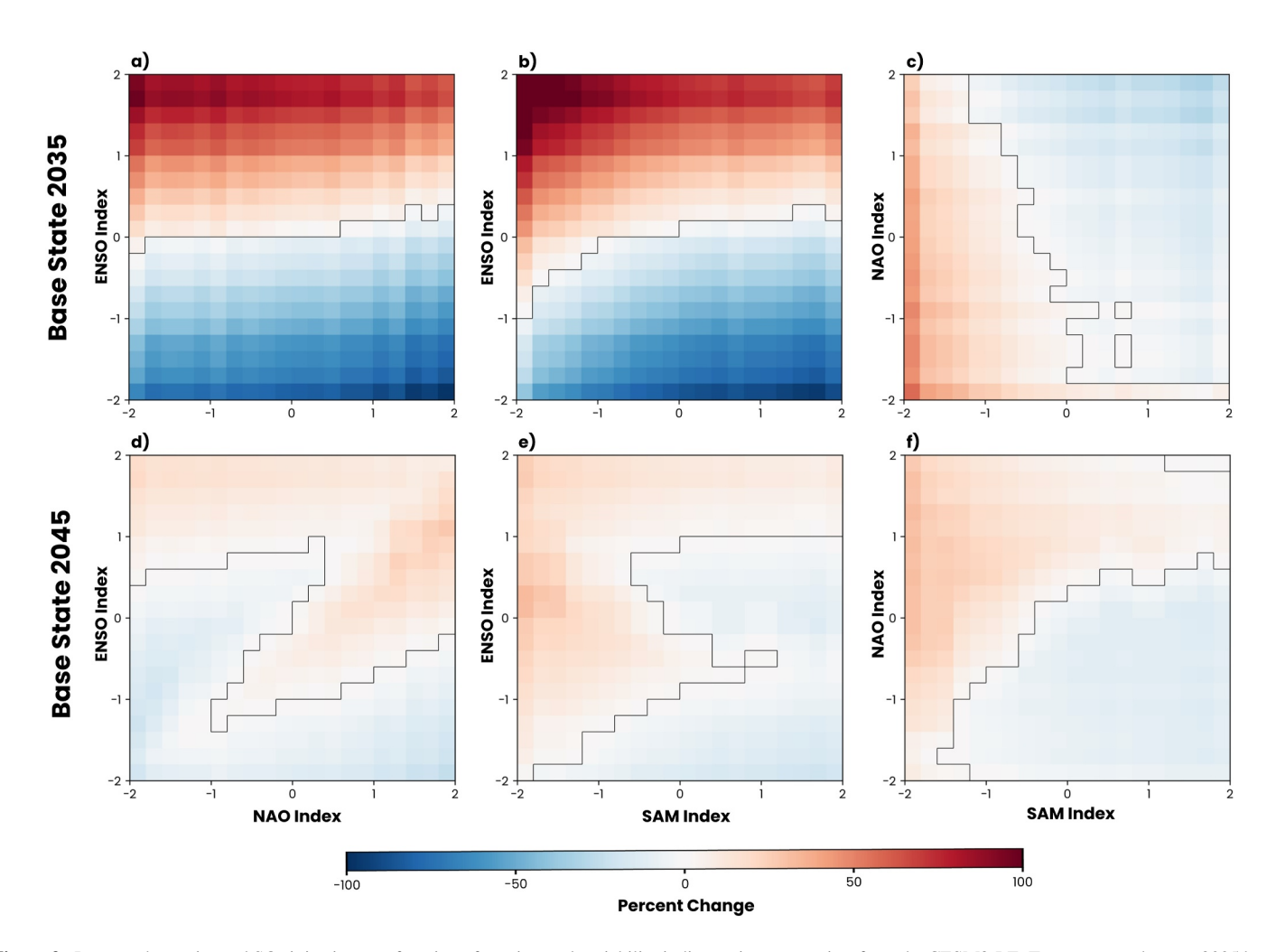


Figure 3. Percent change in total SO_2 injection as a function of two internal variability indices using composites from the CESM2-LE. Top row uses the year 2035 base state and bottom row uses the year 2045 base state. Black line in each panel separates positive percent change (red shading) from negative percent change (blue shading).

patterns. In Figure 2, the base state pattern is the only difference between the green and orange lines in each panel, further demonstrating how the same internal variability pattern can have a different impact on the total SO_2 injection depending on the background state.

Next, in Figure 3, we show how the total SO_2 injection changes as a function of the combination of the two climate indices, with the top row using the 2035 base state and the bottom row using the 2045 base state. Since the controller responds similarly whether anomalies are calculated from ARISE-SAI-CTRL or CESM2-LE data as shown in Figures 2, Figure 3 shows results only using CESM2-LE anomalies. Results using ARISE-SAI-CTRL are in Supporting Information S5. Responses quantified in Figure 2 are also seen in Figure 3, such as the increase in total injection in response to a positive ENSO and a negative SAM. Figure 3 further shows that when these events occur together in 2035, the total injection increases more than when the patterns occur individually. A similar but opposite response is seen when a negative ENSO and a positive SAM occur simultaneously and drive a larger decrease in the total injection.

The impact on the total SO_2 injection from multiple internal variability patterns can change based on the base state (Figure 3). When using the 2035 base state, the largest impacts typically occur when the internal variability events are the strongest, as shown by the largest magnitudes of percent change found in the corners of the top row panels in Figure 3. For a base state year of 2045 (bottom row), we find that the largest magnitude changes no longer necessarily occur when the internal variability events are strongest. For instance, when the NAO is positive, the strongest impact to the total injection occurs when the ENSO index is near one rather than two (Figure 3d). When looking at the T0, T1, and T2 errors for the individual temperature patterns in Figure 3 (see Supporting



23284277, 2024, 6, Downloaded from https://agupubs.onlinelibrary.wiley.com/doi/10.1029/2023EF004300 by Colorado State University, Wiley Online Library on [01/11/2024]. See the

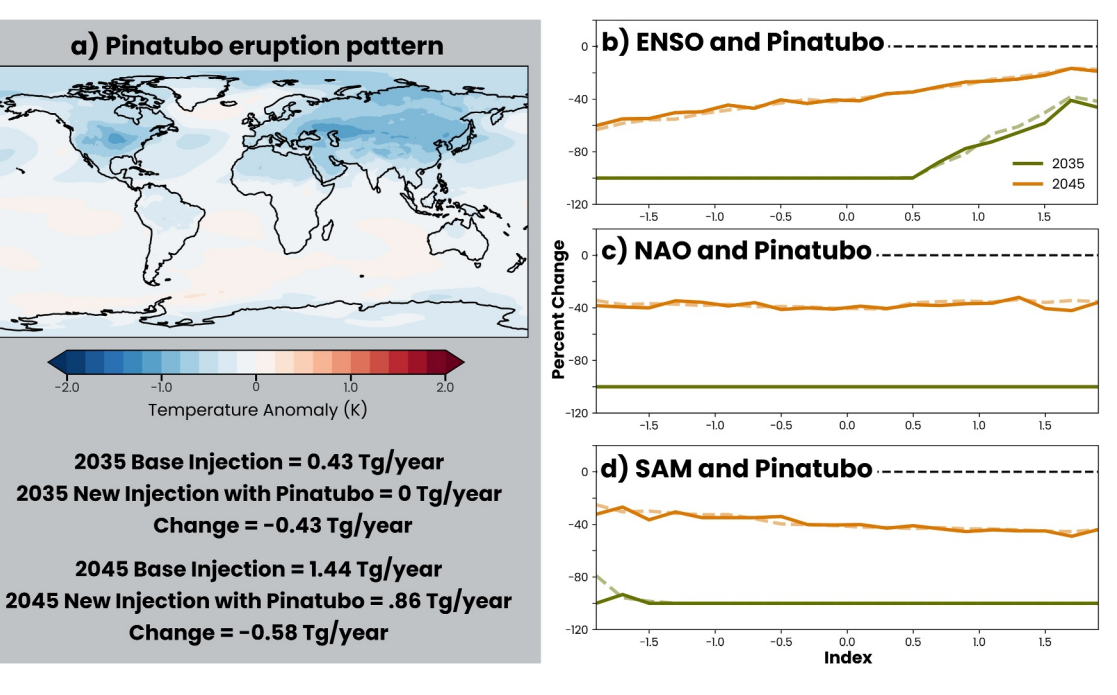


Figure 4. Mt. Pinatubo's impact on the total injection where (a) are the temperature anomalies associated with the Mt. Pinatubo eruption. The injection with Pinatubo is the total SO₂ injected given the base state and the volcano component. Panels (b), (c), and (d) show the percent change in total SO₂ injection as a function of Pinatubo with El-Niño Southern Oscillation, North Atlantic Oscillation, and Southern annular mode respectively. Solid lines use data from ARISE-SAI-CTRL and dashed lines use data from CESM-LE. Green lines use the 2035 base state and orange lines use the 2045 base state. Black dashed line marks zero percent change.

Information S1 in the Figure S6), the sign of the T1 error relative to the T1 target (0.8767) changes sign from negative in 2035 to positive in 2045 while the sign of T0 and T2 errors stay the same. The T1 value describes the north-south temperature gradient where a positive T1 value means the Northern Hemisphere is warmer than the Southern Hemisphere. Therefore, the sign change in T1 errors is likely in response to the uneven hemispheric warming that occurs in response to climate change. For more details about how deviations in T0, T1, and T2 change the total SO₂ injection see Figure S7 in the Supporting Information S1.

We now explore the controller sensitivity to a volcanic eruption represented by the temperature anomaly pattern associated with the 1,991 Mt. Pinatubo eruption (Figure 4a). Introducing the volcanic eruption temperature pattern to the 2035 and 2045 base states decreases the amount of SO_2 the ARISE-SAI controller injects. When the volcanic pattern is added to the 2035 base state alone, the controller injects nothing and when added to the 2045 base state, the injection decreases by 0.58 Tg/year. The Mt. Pinatubo eruption injected approximately 10 Tg of SO_2 into the stratosphere (Bluth et al., 1992; Wilson et al., 1993) and was estimated to cool the Earth's surface by 0.5°C (Parker et al., 1996). Therefore, a volcanic eruption the size of the Mt Pinatubo eruption would reduce the errors in T_0 and thus decrease the total injection determined by the controller. In 2035, the global cooling in response to a Pinatubo-like eruption is enough to negate all experienced global-mean warming (at least from the controller's perspective), removing the need to inject any additional SO_2 . The amount of SO_2 naturally injected by Mt Pinatubo is not enough to combat the amount of warming experienced in 2045.

Including an internal variability pattern in addition to the Mt. Pinatubo eruption pattern allows for the quantification of how much a Pinatubo-like eruption in combination with internal variability impacts the controller-determined SO_2 injection (Figures 4b, 4c, and 4d). In 2035, when a Pinatubu-like eruption removes the need to inject SO_2 , only an ENSO event stronger than 0.5 forces the controller to inject. Warming associated with a positive ENSO greater than 0.5 is enough to cause the ARISE-SAI controller to inject despite the volcanic eruption.

In 2045, when the controller input also contains a single internal variability pattern, a Pinatubo-like eruption decreases the total injection by about 40% as shown by the orange line in Figure 4 centered around -40% rather than around 0% as it is in Figure 2. Additionally, the slope of the orange lines in Figure 4 are smaller than the slopes of the orange lines in Figure 2 indicating that internal variability has a smaller impact on the total injection



when occurring alongside a Pinatubo-like eruption. In summary, a volcanic eruption the size of Pinatubo in 2035 can reduce the total SO_2 injection by 100% except when the ENSO index is greater than 0.5. In 2045, a volcanic eruption of the same size can reduce the total SO_2 injection by about 40% and lessen the impacts of ENSO, NAO, and SAM on total injection amounts.

4. Discussion

By design, controllers respond to variability of a system and therefore work well in systems with uncertainty (Jarvis & Leedal, 2012). However, a controller's ability to respond and impact internal variability can result in complicated feedbacks where the controller can amplify or attenuate the frequency of internal variability, a feature explored thoroughly in MacMartin et al. (2014). These features of a controller are considered and balanced during the tuning phase of a controller. While this may present a challenge toward implementing a control algorithm in reality, Kravitz et al. (2014) showed that a control algorithm designed in one model could be used to meet the targets in a different model, demonstrating the controller's ability to generalize to different systems. The results in this work show a way to quantify a controller's sensitivities to a variety of temperature patterns post tuning, including to those outside of the system used to tune the control algorithm. While the method produces some climate states that may have statistically low chances of occurring or that may never occur, it allows for quick and cheap quantification of internal variability's impact on the total injection determined by the controller. Results in this work are confined to the 2035 and 2045 base states calculated from the ARISE-SAI control simulations (i.e., temperature patterns are from the system the controller was tuned for). Given that this work shows that the internal variability's impact on the total injection depends on the background warming, using a different emissions scenario or model for the base state may result in different quantified sensitivities.

Once sensitivities are quantified, one can consider whether the magnitude in which different internal variability patterns impact the total injection is acceptable. For example, consider the ARISE-SAI controller's response to a Pinatubo-like eruption. The controller injects less when there are naturally occurring aerosols cooling the planet. However, in regards to patterns of internal variability, is it acceptable that more SO₂ is injected when the atmospheric-ocean system is in an El Niño phase rather than a La Niña phase? Or should there be focus on ways to ensure that the majority of the SO₂ injection is in response to climate warming signal alone? Doing so would require the ability to separate the forced and unforced response in our current atmosphere or to predict them with considerable accuracy. Given that knowing or predicting the forced or unforced response with high accuracy is an ongoing area of research (Dai et al., 2015; Mariotti et al., 2018; Xu & Darve, 2022), implementing current methods to determine these responses would introduce further uncertainty into the feedback system.

5. Conclusions

This work quantifies the ARISE-SAI controller sensitivity to internal variability and demonstrates a method that allows for a quick and effective quantification of controller sensitivity post tuning. The ARISE-SAI controller's response to patterns of internal variability associated with ENSO, NAO and SAM as well as a Pinatubo-like eruption are quantified as these patterns cover Northern Hemisphere, Southern Hemisphere, and global temperature impacts. Focus is placed on quantifying these patterns of internal variability in relation to years 2035 and 2045, which correspond to the deployment year in ARISE-SAI and the deployment year in delayed start, respectively (MacMartin et al., 2022). Using these two base state years, we show that internal variability's impact on the total injection is dependent on the background warming it is occurring under. Using this method to explore and quantify sensitivities of a tuned controller provides the opportunity to explore controller responses to a system it is not tuned for, facilitates sensitivity comparisons between scenarios and earth system models, and may promote discussion about the extent to which an SAI-controller responds to variability internal to the climate system.

Data Availability Statement

The CESM2-LE is available at (Danabasoglu et al., 2021). The ARISE-SAI control simulation is available at (Mills et al., 2022). Code used in this work can be found at (Connolly, 2024a) and the processed data is available at (Connolly, 2024b).



Acknowledgments

This work was supported by Defense Advanced Research Projects Agency (DARPA) Grant number HR00112290071. The views expressed here do not necessarily reflect the positions of the U.S. government.

References

- Angell, J. K. (1990). Variation in global tropospheric temperature after adjustment for the El Nino influence, 1958-89. Geophysical Research Letters, 17(8), 1093–1096. https://doi.org/10.1029/gl017i008p01093
- Astrom, K. J., & Murray, R. M. (2021). Feedback systems: An introduction for scientists and engineers. Princeton university press.
- Bluth, G. J., Doiron, S. D., Schnetzler, C. C., Krueger, A. J., & Walter, L. S. (1992). Global tracking of the SO2 clouds from the June, 1991 Mount Pinatubo eruptions. *Geophysical Research Letters*, 19(2), 151–154. https://doi.org/10.1029/91g102792
- Cicerone, R. J. (2006). Geoengineering: Encouraging research and overseeing implementation. Climate Change, 77(3), 221–226. https://doi.org/10.1007/s10584-006-9102-x
- Connolly, C. (2024a). Code accompanying quantifying the impact of internal variability on the CESM2 control algorithm for stratospheric aerosol injection [Software]. Zenodo. https://zenodo.org/doi/10.5281/zenodo.10914568
- Connolly, C. (2024b). Data from: Quantifying the impact of internal variability on the CESM2 control algorithm for stratospheric aerosol injection dataset [Dataset]. Dryad. https://doi.org/10.5061/dryad.66t1g1k7v
- Crutzen, P. J. (2006). Albedo enhancement by stratospheric sulfur injections: A contribution to resolve a policy dilemma? *Climate Change*, 77(3–4), 211–220. https://doi.org/10.1007/s10584-006-9101-y
- 4), 211–220. https://doi.org/10.1007810384-006-9101-y
 Dai, A., Fyfe, J. C., Xie, S.-P., & Dai, X. (2015). Decadal modulation of global surface temperature by internal climate variability. *Nature Climate Change*, 5(6), 555–559. https://doi.org/10.1038/nclimate2605
- Danabasoglu, G., Deser, K. B., Rodgers, C., & Timmermann, A. (2021). CESM2 large ensemble. [Dataset]. https://doi.org/10.5194/esd-12-1393-
- Danabasoglu, G., Lamarque, J.-F., Bacmeister, J., Bailey, D. A., DuVivier, A. K., Edwards, J., et al. (2020). The community earth system model version 2 (CESM2). *Journal of Advances in Modeling Earth Systems*, 12(2). https://doi.org/10.1029/2019ms001916
- Deser, C., Phillips, A., Bourdette, V., & Teng, H. (2012). Uncertainty in climate change projections: The role of internal variability. *Climate Dynamics*, 38(3), 527–546. https://doi.org/10.1007/s00382-010-0977-x
- Diao, C., Barnes, E. A., & Hurrell, J. W. (2023). Influence of ENSO on stratospheric sulfur dioxide injection in the CESM2 ARISE-SAI-1.5 simulations. *Authorea Preprints*. Retrieved from https://essopenarchive.org/users/631510/articles/650823-influence-of-enso-on-stratospheric-sulfur-dioxide-injection-in-the-cesm2-arise-sai-1-5-simulations
- Fogt, R. L., & Marshall, G. J. (2020). The southern annular mode: Variability, trends, and climate impacts across the southern hemisphere. Wiley interdisciplinary reviews Climate change, 11(4). https://doi.org/10.1002/wcc.652
- Fuentes-Franco, R., Docquier, D., Koenigk, T., Zimmermann, K., & Giorgi, F. (2023). Winter heavy precipitation events over northern Europe modulated by a weaker NAO variability by the end of the 21st century. npj Climate and Atmospheric Science, 6(1), 1–9. https://doi.org/10.1038/s41612-023-00396-1
- Gillett, N. P., Kell, T. D., & Jones, P. (2006). Regional climate impacts of the southern annular mode. *Geophysical Research Letters*, 33(23). https://doi.org/10.1029/2006g1027721
- Hanna, E., & Cropper, T. E. (2017). North Atlantic oscillation. In Oxford research encyclopedia of climate science.
- Ho, M., Kiem, A., & Verdon-Kidd, D. (2012). The southern annular mode: A comparison of indices. Hydrology and Earth System Sciences, 16(3), 967–982. https://doi.org/10.5194/hess-16-967-2012
- Holasek, R., Self, S., & Woods, A. (1996). Satellite observations and interpretation of the 1991 Mount Pinatubo eruption plumes. *Journal of Geophysical Research*, 101(B12), 27635–27655. https://doi.org/10.1029/96jb01179
- Hurrell, J. W. (1996). Influence of variations in extratropical wintertime teleconnections on northern hemisphere temperature. Geophysical Research Letters, 23(6), 665–668. https://doi.org/10.1029/96g100459
- Hurrell, J. W., & Deser, C. (2010). North Atlantic climate variability: The role of the North Atlantic oscillation. *Journal of Marine Systems*, 79(3), 231–244. https://doi.org/10.1016/j.jmarsys.2009.11.002
- Jarvis, A., & Leedal, D. (2012). The geoengineering model intercomparison project (GeoMIP): A control perspective. Atmospheric Science Letters, 13(3), 157–163. https://doi.org/10.1002/asl.387
- Kravitz, B., Caldeira, K., Boucher, O., Robock, A., Rasch, P. J., Alterskjaer, K., et al. (2013). Climate model response from the geoengineering model intercomparison project (GeoMIP). *Journal of Geophysical Research: Atmospheres*, 118(15), 8320–8332. https://doi.org/10.1002/jgrd.
- Kravitz, B., MacMartin, D. G., Leedal, D. T., Rasch, P. J., & Jarvis, A. J. (2014). Explicit feedback and the management of uncertainty in meeting climate objectives with solar geoengineering. Environmental Research Letters, 9(4), 044006. https://doi.org/10.1088/1748-9326/9/4/044006
- Kravitz, B., MacMartin, D. G., Mills, M. J., Richter, J. H., Tilmes, S., Lamarque, J.-F., et al. (2017). First simulations of designing stratospheric sulfate aerosol geoengineering to meet multiple simultaneous climate objectives. *Journal of Geophysical Research: Atmospheres*, 122(23), 12–616. https://doi.org/10.1002/2017jd026874
- Kravitz, B., Robock, A., Tilmes, S., Boucher, O., English, J. M., Irvine, P. J., et al. (2015). The geoengineering model intercomparison project phase 6 (GeoMIP6): Simulation design and preliminary results. *Geoscientific Model Development*, 8(10), 3379–3392. https://doi.org/10.5194/gmd-8-3379-2015
- Liu, P. R., & Raftery, A. E. (2021). Country-based rate of emissions reductions should increase by 80% beyond nationally determined contributions to meet the 2°c target. Communications Earth & Environment, 2(1), 29. https://doi.org/10.1038/s43247-021-00097-8
- MacMartin, D. G., Kravitz, B., Keith, D. W., & Jarvis, A. (2014). Dynamics of the coupled human-climate system resulting from closed-loop control of solar geoengineering. Climate Dynamics, 43(1), 243–258. https://doi.org/10.1007/s00382-013-1822-9
- MacMartin, D. G., Visioni, D., Kravitz, B., Richter, J. H., Felgenhauer, T., Lee, W. R., et al. (2022). Scenarios for modeling solar radiation modification. *Proceedings of the National Academy of Sciences of the United States of America*, 119(33), e2202230119. https://doi.org/10.1073/pnas.2202230119
- Mariotti, A., Ruti, P. M., & Rixen, M. (2018). Progress in subseasonal to seasonal prediction through a joint weather and climate community effort. npj Climate and Atmospheric Science, 1(1), 1–4. https://doi.org/10.1038/s41612-018-0014-z
- Mills, M. J., Visioni, D., & Richter, J. (2022). CESM2-waccm6-ssp245 [Dataset]. UCAR/NCAR-CISL-CDP. https://doi.org/10.26024/0cs0-ev98 NASEM. (2021). Reflecting sunlight: Recommendations for solar geoengineering research and research governance. National Academies Press.
- Parker, D. E., Wilson, H., Jones, P. D., Christy, J. R., & Folland, C. K. (1996). The impact of Mount Pinatubo on world-wide temperatures. *Journal of Applied Meteorology and Climatology*, 16(5), 487–497. https://doi.org/10.1002/(sici)1097-0088(199605)16:5<487::aid-joc39>3.0.co;2-j
- Raftery, A. E., Zimmer, A., Frierson, D. M. W., Startz, R., & Liu, P. (2017). Less than 2°C warming by 2100 unlikely. *Nature Climate Change*, 7(9), 637–641. https://doi.org/10.1038/nclimate3352
- Rasch, P. J., Crutzen, P. J., & Coleman, D. B. (2008). Exploring the geoengineering of climate using stratospheric sulfate aerosols: The role of particle size. Geophysical Research Letters, 35(2). https://doi.org/10.1029/2007gl032179





- 10.1029/2023EF004300
- Riahi, K., van Vuuren, D. P., Kriegler, E., Edmonds, J., O'Neill, B. C., Fujimori, S., et al. (2017). The shared socioeconomic pathways and their energy, land use, and greenhouse gas emissions implications: An overview. *Global Environmental Change*, 42, 153–168. https://doi.org/10.1016/j.gloenvcha.2016.05.009
- Richter, J. H., Visioni, D., MacMartin, D. G., Bailey, D. A., Rosenbloom, N., Dobbins, B., et al. (2022). Assessing responses and impacts of solar climate intervention on the earth system with stratospheric aerosol injection (ARISE-SAI): Protocol and initial results from the first simulations. Geoscientific Model Development, 15(22), 8221–8243. https://doi.org/10.5194/gmd-15-8221-2022
- Riviére, G., & Drouard, M. E. (2015). Understanding the contrasting North Atlantic oscillation anomalies of the winters of 2010 and 2014. Geophysical Research Letters, 42(16), 6868–6875. https://doi.org/10.1002/2015g1065493
- Rodgers, K. B., Lee, S.-S., Rosenbloom, N., Timmermann, A., Danabasoglu, G., Deser, C., et al. (2021). Ubiquity of human-induced changes in climate variability. *Earth System Dynamics*, 12(4), 1393–1411. https://doi.org/10.5194/esd-12-1393-2021
- Tilmes, S., Richter, J. H., Kravitz, B., MacMartin, D. G., Mills, M. J., Simpson, I. R., et al. (2018). CESM1(WACCM) stratospheric aerosol geoengineering large ensemble project. *Bulletin of the American Meteorological Society*, 99(11), 2361–2371. https://doi.org/10.1175/bams-d-17-0267.1
- Trenberth, K. E. (1997). The definition of El Niño. Bulletin of the American Meteorological Society, 78(12), 2771–2778. https://doi.org/10.1175/1520-0477(1997)078<2771:tdoeno>2.0.co;2
- Wilson, J., Jonsson, H., Brock, C., Toohey, D., Avallone, L., Baumgardner, D., et al. (1993). In situ observations of aerosol and chlorine monoxide after the 1991 eruption of Mount Pinatubo: Effect of reactions on sulfate aerosol. *Science*, 261(5125), 1140–1143. https://doi.org/10.1126/science.261.5125.1140
- Xu, K., & Darve, E. (2022). Physics constrained learning for data-driven inverse modeling from sparse observations. *Journal of Computational Physics*, 453, 110938. https://doi.org/10.1016/j.jcp.2021.110938

